**Supporting Information**

# Synergistic Melamine intercalation and $Zn(NO_3)_2$ Activation to N-doped porous carbon supported $Fe/Fe_3O_4$ for efficient electrocatalytic oxygen reduction

*Yaoyao Ni[a], Tingjuan Wang[a], Yan Zhou[a], Chao Wang[a], Yingwen Tang[b], Tao Li[c] and Baoyou Geng*[a,d]*

[a]College of Chemistry and Materials Science, The Key Laboratory of Electrochemical Clean Energy of Anhui Higher Education Institutes, Anhui Provincial Engineering Laboratory for New-Energy Vehicle Battery Energy-Storage Materials, Anhui Normal University, No.189 Jiuhua South Road, Wuhu, 241002, China.

[b]College of Physics and Information Engineering, Minnan Normal University

[c]Shanghai Institute of Technical Physics, Chinese Academy of Sciences

[d]Institute of Energy, Hefei Comprehensive National Science Center, Anhui, Hefei, 230031, China.

*Corresponding Author: bygeng@mail.ahnu.edu.cn

## 1. Additional Figures

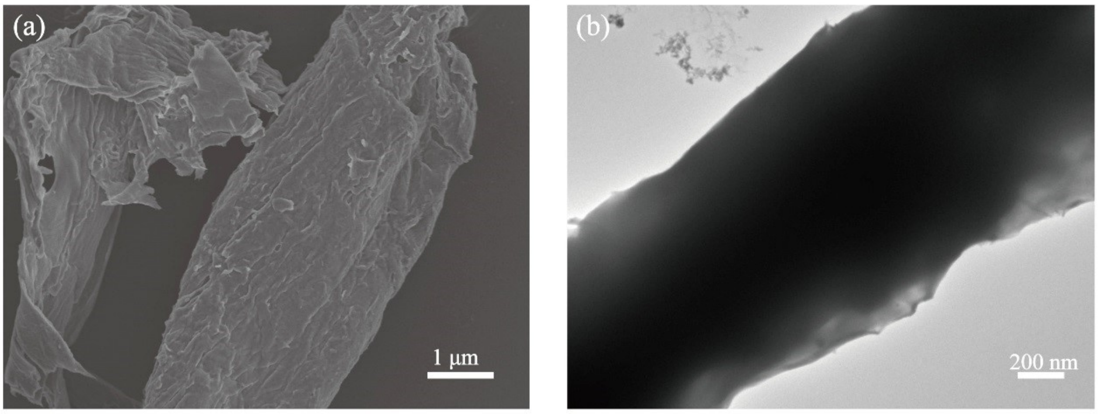


**Fig. S1** SEM and TEM images of unactivated α-cellulose powder.

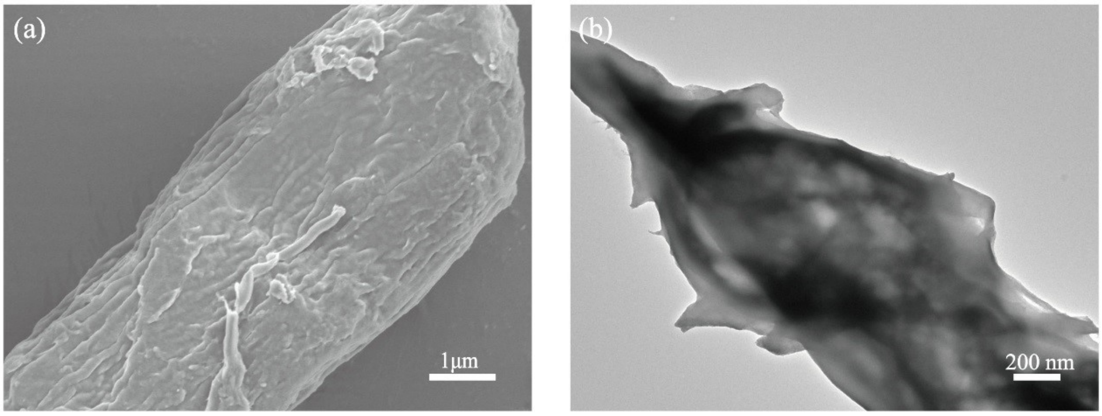


**Fig. S2** SEM and TEM images of $Fe/Fe_3O_4$@NC catalyst precursor powder.

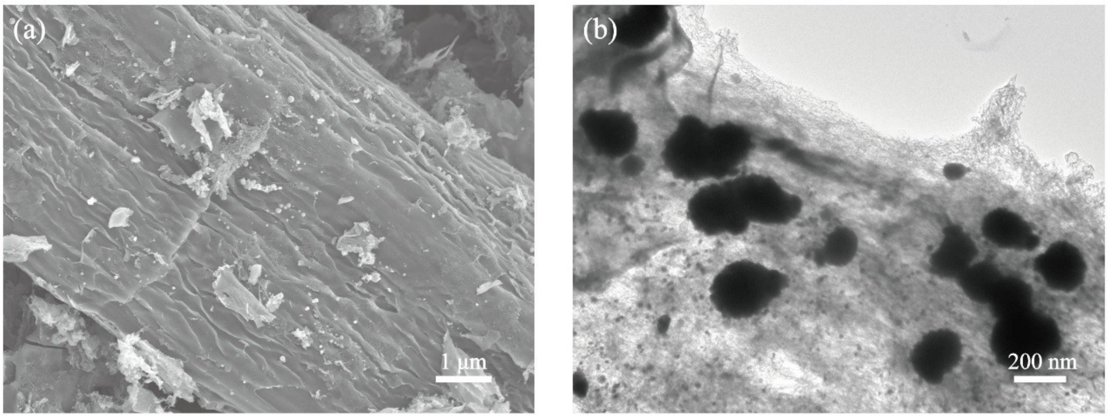


**Fig. S3** SEM and TEM images of materials prepared by urea as nitrogen source.

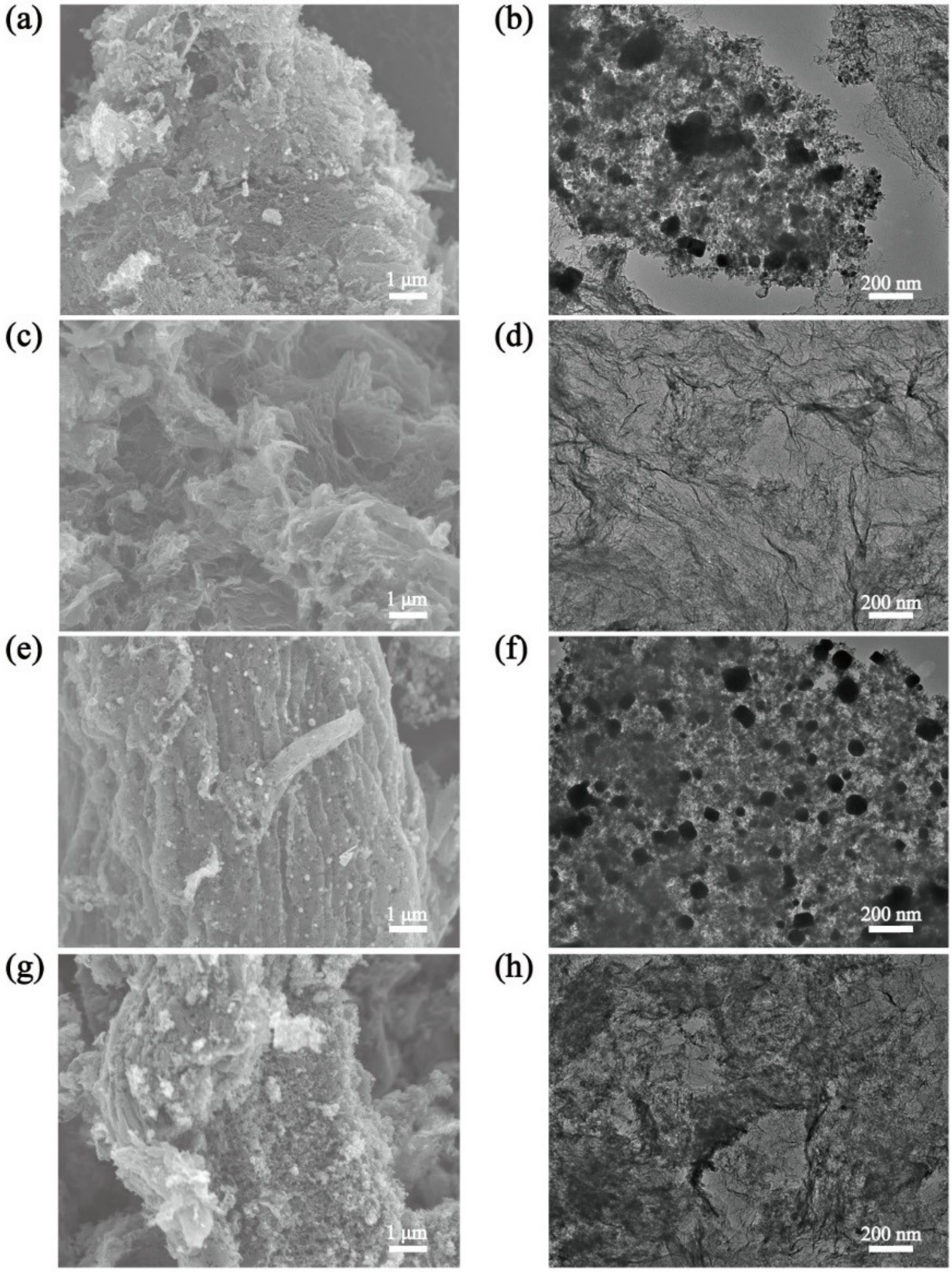


**Fig. S4** SEM and TEM images of $Fe/Fe_3O_4$@NC (Zn-free) (a, b), NC (Fe-free) (c, d), $Fe/Fe_3O_4$@C (N-free) (e, f) and $Fe_3O_4$@NC (g, h).

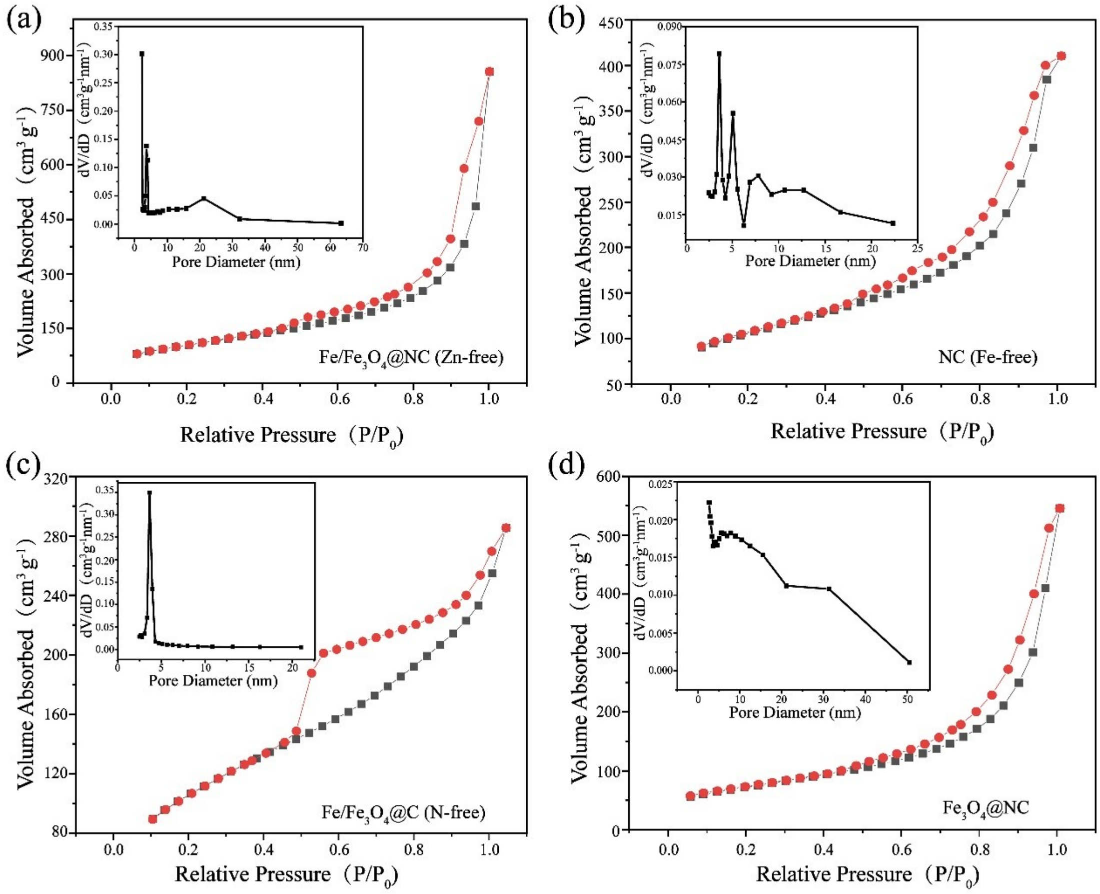


**Fig. S5** $N_2$ adsorptio-desorption isotherm and pore size distribution of Fe/Fe3O4@NC (Zn-free) (a), NC (Fe-free) (b), $Fe/Fe_3O_4@C$ (N-free) (c) and $Fe_3O_4@NC$ (d) catalysts.

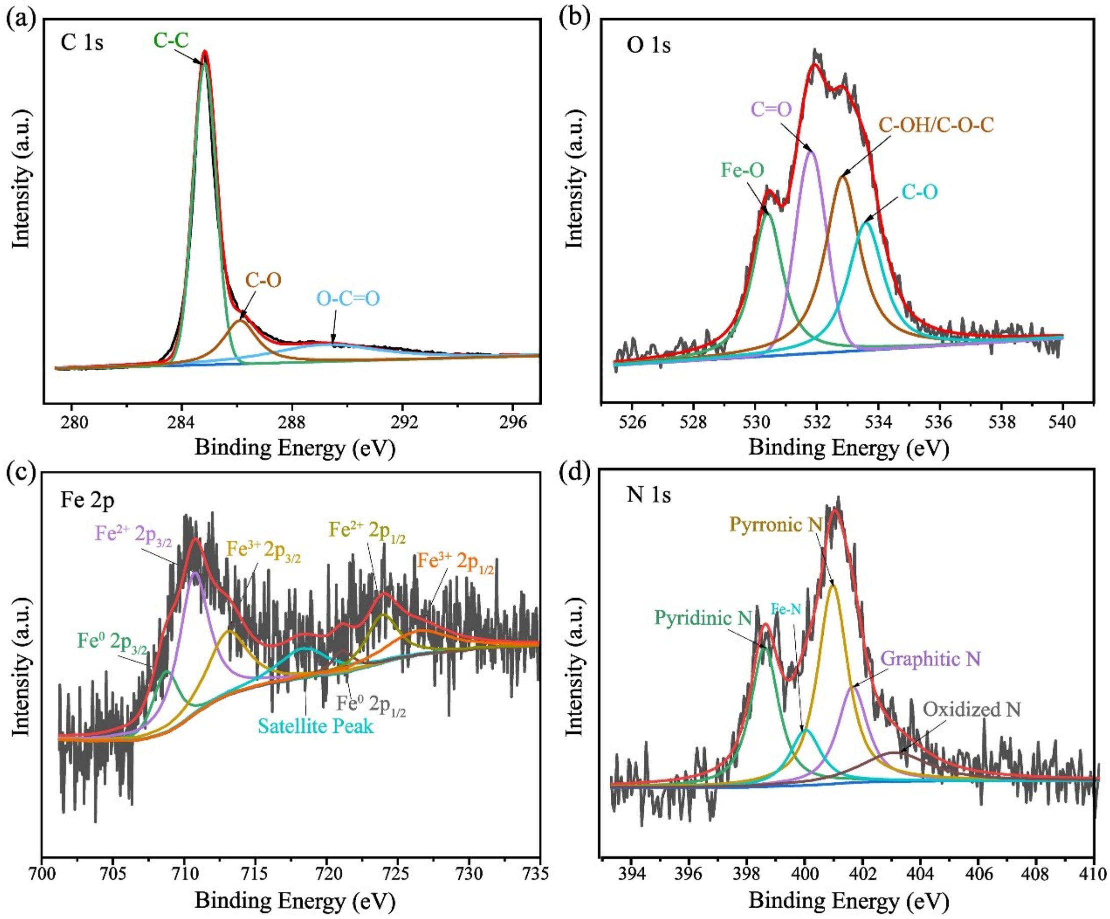


**Fig. S6** XPS spectrum of (a) C 1s, (b) O 1s in $Fe/Fe_3O_4$@C(N-free), XPS spectrum of (c) Fe 2p, (d) N 1s in $Fe/Fe_3O_4$@C (Zn-free).

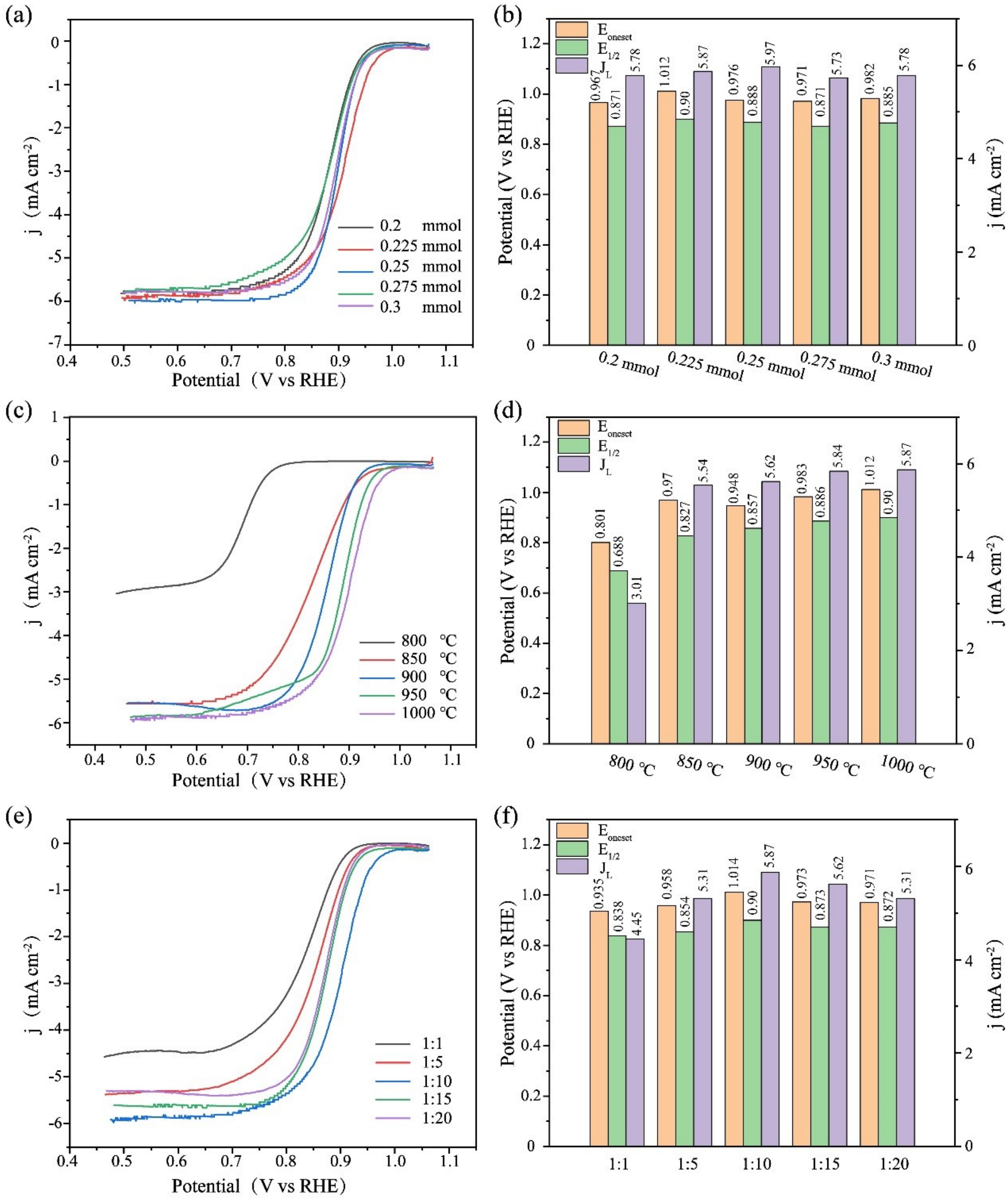


**Fig. S7** LSV curves at 1600 rpm and the corresponding bar graph of the $Fe/Fe_3O_4$@NC electrocatalysts under different Fe content (a, b), pyrolysis temperature (c, d) and mass ratio of the precursor powder to melamine (e, f) in 0.1 M KOH solution at a scan rate of 5 mV $s^{-1}$.

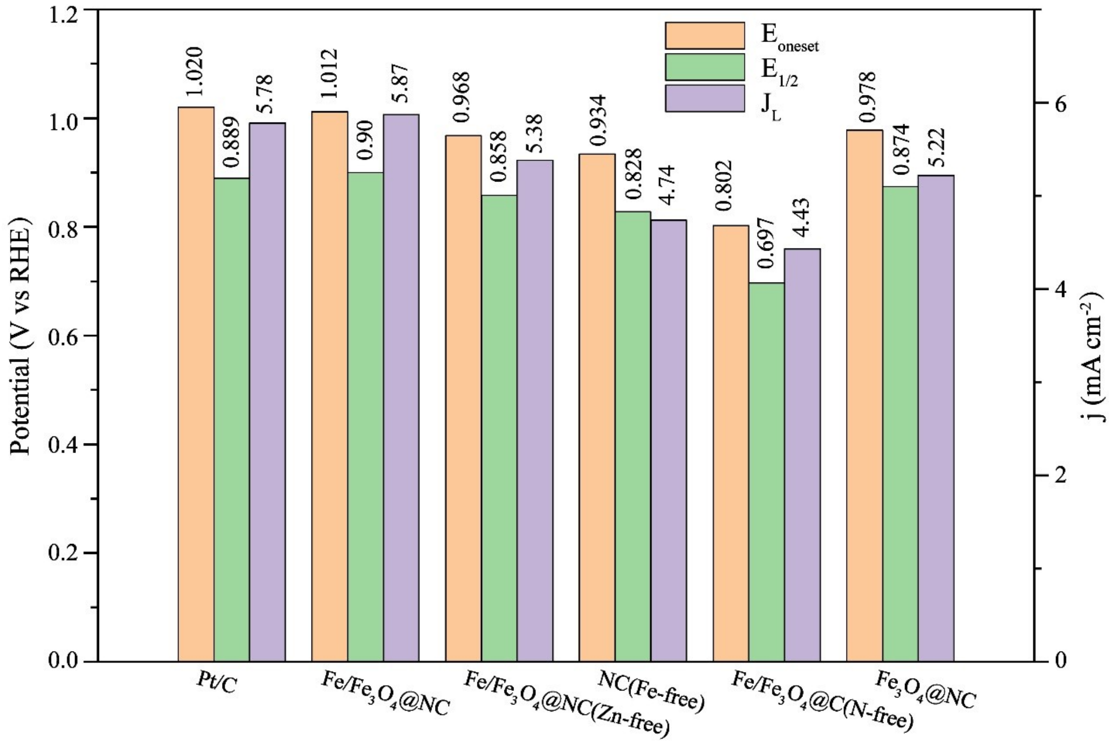


**Fig. S8** The corresponding bar graph of the $E_{1/2}$, Eoneset and $J_L$ of Pt/C, $Fe/Fe_3O_4$@NC, $Fe/Fe_3O_4$@NC (Zn-free), $Fe/Fe_3O_4$@NC (N-free), NC (Fe-free) and $Fe_3O_4$@NC catalysts, respectively.

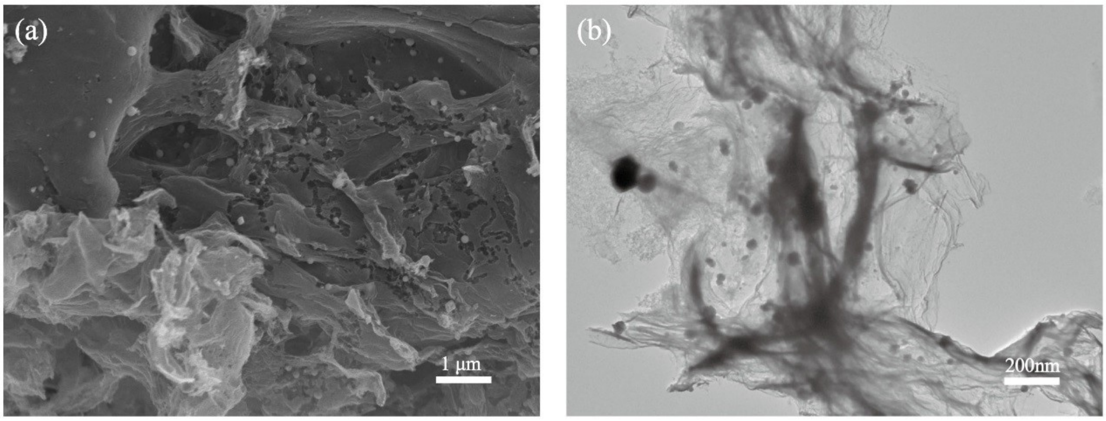


**Fig. S9** SEM and TEM images of $Fe/Fe_3O_4$@NC catalyst after 5,000 CV cycles of ADT test.

## 2. Additional Tables

**Table S1.** Pore structure properties from BET analysis of $Fe/Fe_3O_4$@NC, $Fe/Fe_3O_4$@NC (Zn-free).

| Samples | BET surface area ($m^2\ g^{-1}$) | $V_{total}$ ($cm^3\ g^{-1}$)[a] | $V_{micro}$ ($cm^3\ g^{-1}$)[b] | $V_{meso}$ ($cm^3\ g^{-1}$)[c] | Mesopore volume ratio (%) |
|---|---|---|---|---|---|
| $Fe/Fe_3O_4$@NC | 546.70 | 1.4147 | 0.0359 | 1.3788 | 97.46 |
| $Fe/Fe_3O_4$@NC (Zn-free) | 449.87 | 1.0885 | 0.0339 | 1.0546 | 96.86 |
| NC (Fe-free) | 357.91 | 0.6211 | 0.0388 | 0.5823 | 93.75 |
| $Fe/Fe_3O_4$@C (N-free) | 302.69 | 0.4167 | 0.0752 | 0.3415 | 81.95 |
| $Fe_3O_4$@NC | 242.70 | 0.7276 | 0.0146 | 0.7130 | 97.99 |

NC (Fe-free), $Fe/Fe_3O_4$@C (N-free) and $Fe_3O_4$@NC catalysts.

**Note:**

[a] The total pore volumes ($V_{total}$) were estimated at $P/P_0 = 0.95$.

[b] Micropore volume ($V_{micro}$) were calculated using the t-plot method.

[c] Mesopore volume ($V_{meso}$) were calculated by subtracting $V_{micro}$ from $V_{total}$.

**Table S2.** Comparison of the ORR performance for $Fe/Fe_3O_4$@NC and other Fe-N-C-based catalysts.

| Catalysts | Electrolyte | Performance | Ref. |
|---|---|---|---|
| $Fe/Fe_3O_4$@NC | 0.1 M KOH | $E_{onset}$=1.012 V, $E_{1/2}$=0.90 V, $J_L$=5.876 mA $cm^{-2}$ | **This work** |
| $Fe_3O_4/Fe_3N$/Fe-N-C@PC | 0.1 M KOH | $E_{1/2}$=0.90 V, $J_L$=5.542 mA $cm^{-2}$ | 1 |
| Fe/Fe-N-C | 0.1 M KOH | $E_{1/2}$=0.881 V, $J_L$=5.714 mA $cm^{-2}$ | 2 |
| Fe-N-C | 50 mM PBS solution | $E_{1/2}$=0.842 V, $J_L$=3.14 mA $cm^{-2}$ | 3 |
| Fe-HPC | 0.1 M KOH | $E_{onset}$=0.978 V, $E_{1/2}$=0.85 V | 4 |
| $Zn(NO_3)_2$-Fe/C/N@bio-C | 0.1 M KOH | $E_{onset}$=0.95 V, $E_{1/2}$=0.86 V, $J_L$=6.21 mA $cm^{-2}$ | 5 |
| $ZnCl_2$-Fe/C/N@bio-C | 0.1 M KOH | $E_{onset}$=0.89 V, $E_{1/2}$= 0.77 V, $J_L$=6.20 mA $cm^{-2}$ | 5 |
| Fe-N/C | 0.1 M NaOH | $E_{1/2}$= 0.892 V, $J_L$=4.26 mA $cm^{-2}$ | 6 |
| Fe-N/C-SACs | 0.1 M KOH | $E_{onset}$=0.89 V, $E_{1/2}$= 0.89 V, $J_L$=5.64 mA $cm^{-2}$ | 7 |
| Fe-N-PPC | 0.1 M KOH | $E_{onset}$=0.966 V, $E_{1/2}$= 0.891 V, $J_L$=5.077 mA $cm^{-2}$ | 8 |
| SA-Fe/NHPC | 0.1 M KOH | $E_{1/2}$= 0.87 V, $J_L$=4.1 mA $cm^{-2}$ | 9 |
| $Zn/Fe_{SA}$-PC/950/$NH_3$ | 0.1 M KOH | $E_{onset}$=1.00 V, $E_{1/2}$= 0.88 V | 10 |
| Fe-ISA/NC | 0.1 M KOH | $E_{onset}$=1.00 V, $E_{1/2}$= 0.89 V | 11 |
| Fe-N-$C_{wood}$ | 0.1 M KOH | $E_{onset}$=0.98 V, $E_{1/2}$= 0.90 V | 12 |

## References


1. R. Hao, J. Chen, Z. Wang, J. Zhang, Q. Gan, Y. Wang, Y. Li, W. Luo, Z. Wang, H. Yuan, C. Yan, W. Zheng, W. Huang, P. Liu, J. Yan, K. Liu, C. Liu and Z. Lu, Iron polyphthalocyanine-derived ternary-balanced $Fe_3O_4/Fe_3N$/Fe-N-C@PC as a high-performance electrocatalyst for the oxygen reduction reaction, *Sci. China Mater*, 2021, **64**, 2987-2996.
2. X. Zheng, X. Cao, Z. Sun, K. Zeng, J. Yan, P. Strasser, X. Chen, S. Sun and R. Yang, Indiscrete metal/metal-N-C synergic active sites for efficient and durable oxygen electrocatalysis toward advanced Zn-air batteries, *Appl. Catal, B*., 2020, **272**, 118967.
3. G. Yang, Z. Zhang, X. Kang, L. Li, Y. Li and Y. Sun, Fe-N-C Composite Catalyst Derived from Solid Digestate for the Oxygen Reduction Reaction in Microbial Fuel Cells, *ACS Appl. Energy Mater*, 2020, **3**, 11929-11938.
4. D. Li, Y. Qu, S. Li, M. Wei and Y. Liu, A novel honeycomb Fe-N-C composition derived from wheat flour as an efficiency catalyst for the oxygen reduction reaction, *J. Solid State Electrochem*, 2020, **24**, 1105-1112.
5. Y. Li, H. Hu, J. Song, Y. Wu, X. Lv, Z. Xiao, F. Wang and Y. Chen, An Excellent Fe, N Co-Doped Porous Biomass Carbon Oxygen Reduction Reaction Electrocatalyst: Effect of Zinc-Based Activators on Catalytic Activity, *Energy Technol*, 2020, **8**, 2194-4296.
6. Q. Wu, D. Deng, Y. He, Z. Zhou, S. Sang and Z Zhou, Fe/N-doped mesoporous carbons derived from soybeans: A highly efficient and low-cost non-precious metal catalyst for ORR, *J. Cent. South Univ*, 2020, **27**, 344-355.
7. D. Wu, W. Liu, J. Hu, C. Zhu, H. Jing, J. Zhang, C. Hao and Y. Shi, Direct transformation of raw biomass into a Fe-Nx-C single-atom catalyst for efficient oxygen reduction reaction, *Mater. Chem. Front*, 2021, **5**, 3093-3098.
8. Y. Wang, M. Zhu, G. Wang, B. Dai, F. Yu, Z. Tian and X. Guo, Enhanced Oxygen Reduction Reaction by In Situ Anchoring Fe(2)N Nanoparticles on Nitrogen-Doped Pomelo Peel-Derived Carbon, *Nanomater. (Basel)*, 2017, **7**, 2079-4991.
9. Z. Zhang, X. Gao, M. Dou, J. Ji and F. Wang, Biomass Derived N-Doped Porous Carbon Supported Single Fe Atoms as Superior Electrocatalysts for Oxygen Reduction, *Small*, 2017, **13**, 1604290.
10. H. S. Kim, J. Lee, J.-H. Jang, H. Jin, V. K. Paidi, S.-H. Lee, K.-S. Lee, P. Kim and S. J. Yoo, Waste pig blood-derived 2D Fe single-atom porous carbon as an efficient electrocatalyst for zinc-air batteries and AEMFCs, *Appl. Surf. Sci*, 2021, **563**, 150208.
11. Wang X, Du J, Zhang Q, Gu L, Cao L, Liang H-P. In situ synthesis of sustainable highly efficient single iron atoms anchored on nitrogen doped carbon derived from renewable biomass, Carbon., 2020, 157, 14-621.
12. D. Li, Z, Han, K. Leng, S. Ma, Y. Wang and J. Bai, Biomass wood-derived efficient Fe–N–C catalysts for oxygen reduction reaction, *J. Mater. NanoSci*, 2021, **56**, 12764-12774.